# Supporting Information

**Fabrication of Sub-1 nm Gap Electrodes Using Metal-Mask Patterning and Conductivity Measurements of Molecules in Nanoscale Spaces**

Yasuhisa Naitoh*[a], Ken Albrecht[b,c], Qingshuo Wei[d], Kimihisa Yamamoto[b,c], Hisashi Shima[a] and Takao Ishida[d]

[a]Nanoelectronics Research Institute, Department of Electronics and Manufacturing, National Institute of Advanced Industrial Science and Technology (AIST), Higashi 1-1-1, Tsukuba, Ibaraki 305-8562, Japan. E-mail: ys-naitou@aist.go.jp

[b]Laboratory for Chemistry and Life Science, Tokyo Institute of Technology, Nagatsuta 4259, Midori-ku, Yokohama 226-8503, Japan.

[c]JST, ERATO Yamamoto Atom Hybrid Project, Nagatsuta 4259, Midori-ku, Yokohama, 226-8503, Japan.

[d]Nanomaterials Research Institute, Department of Materials and Chemistry, National Institute of Advanced Industrial Science and Technology (AIST), Higashi 1-1-1, Tsukuba, Ibaraki 305-8562, Japan.

Table of Contents

## 1. *I–V* Curve Fitting Using the Single-Level Tunneling Transport Model

In this study, the *I–V* characteristics of nanogap electrodes after immersion in 1,4-benzenedithiol (BDT) solution were investigated using the single-level tunneling transport model.[1,2] In this model, the observed current $I(V)$ is given by

$$I(V) = N\frac{8e}{h}\frac{\Gamma_L\Gamma_R}{\Gamma_L+\Gamma_R}\left\{\tan^{-1}\left(\frac{\frac{\Gamma_R}{\Gamma_L+\Gamma_R}eV-\varepsilon_0}{\Gamma_L+\Gamma_R}\right)+\tan^{-1}\left(\frac{\frac{\Gamma_L}{\Gamma_L+\Gamma_R}eV+\varepsilon_0}{\Gamma_L+\Gamma_R}\right)\right\}, \quad (2)$$

where $N$ is the number of BDT molecules, $\varepsilon_0$ is the energy of the molecular orbital involved in the charge-transfer process, and $\Gamma_L$ and $\Gamma_R$ are the coupling strengths between the molecular wire and the left and right Au electrodes, respectively. S. Kaneko *et al.* used this model to fit the experimental *I–V* curves measured using the mechanically controlled break-junction method,[2] in which the number of bridged molecular wires can be controlled. They investigated a single bridged BDT molecule (Fig. S1a), and $N$ was defined as 1. However, in this study, because the number of BDT molecules was unclear, $N$ was added to Eq. (2). The integral number of $N$ was calculated by dividing the observed conductance by the conductance of a single BDT molecule. When $N$ was below 1, $N$ was defined as 1.

According to the strict definition, because the conductance of a single Au–BDT–Au junction varies from $10^{-4}G_0$ to $0.1G_0$ under different experimental conditions[2-10], this $N$ is not accurate bridging BDT number but the smallest bridging number which can be considered. Moreover, each Au–BDT–Au junction which is contains of nonbridging junction like as Fig. S1c has individual values of $\varepsilon_0$, $\Gamma_L$, and $\Gamma_R$. Even if a nanogap electrode contains stable Au–BDT–Au junctions, the electrode will contain a mixture of bridging parts, as in Fig. S1b, and nonbridging parts, as in Fig. S1c. Therefore, the addition of term $N$ is not reflected in the actual BDT number.

Because one side of coupling energy of nonbridging Au–BDT–Au junction is quite smaller than that of bridging Au–BDT–Au junction, large differences in conductance are expected between bridging and nonbridging Au–BDT–Au junctions. We assumed that the observed conductance preferentially contains of the contribution of bridging parts if the observed electrode had mixtures of the configurations shown in Fig. S1b and S1c. In addition, the distribution of $\varepsilon_0$ has a single peak in three types of high-, middle-, and low-conductance Au–BDT–Au junction and coupling of $\Gamma_L$ and $\Gamma_R$ has an individual single peak with the three types of that in the previously study[2]. Therefore, it is expected that fitting parameters of the largest conductance condition are preferentially estimated from experimental *I–V* curves. Using this assumption, we fitted the observed current using the single-level tunneling transport model [Eq. (2)].

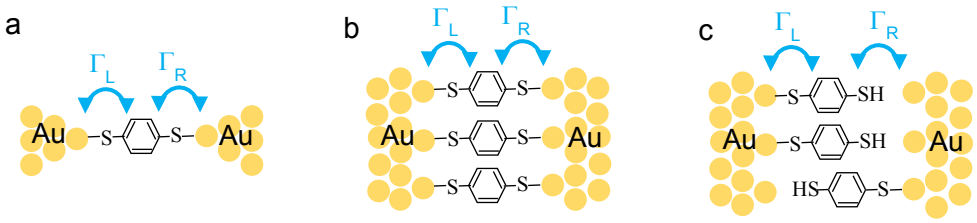


**Fig. S1.** Schematics of Au–BDT–Au junctions: single bridging (a), bridging (b), and nonbridging (c).

## 2. Dependence of Fitting Parameters on *N*

Fig. S2a and S2b show the typical experimental and fitted *I*–*V* curves of BDT conductance obtained using the nanogap electrodes fabricated with process voltages of 8 and 16 V, respectively. These figures are the same as Fig. 4a and 4b. In the fitted curves, *N* was set at 8 and 1 for the process voltages of 8 and 16 V, respectively. However, accurate BDT numbers are not unclear and might be different to accurate BDT number as mentioned above. If bridging BDT contains lower conductance bridging, actual bridging number will be larger than *N*. In addition, when all BDT molecules are not bridged, as in Figure S1(c), the number of BDT molecules affecting the *I*–*V* curve is large. Fig. S2c shows the dependences of the fitting parameters on *N*. The fitting parameters were estimated from the *I*–*V* curves shown in Fig. S2a and S2b using the single-level tunneling transport model (Eq. (2)). $\Gamma$ clearly decreased when *N* increased, whereas $\varepsilon_0$ hardly changed with *N*. This indicates that the value of $\varepsilon_0$ is reliable regardless of the value of *N* used. Therefore, we mainly discussed $\varepsilon_0$ in the main article.

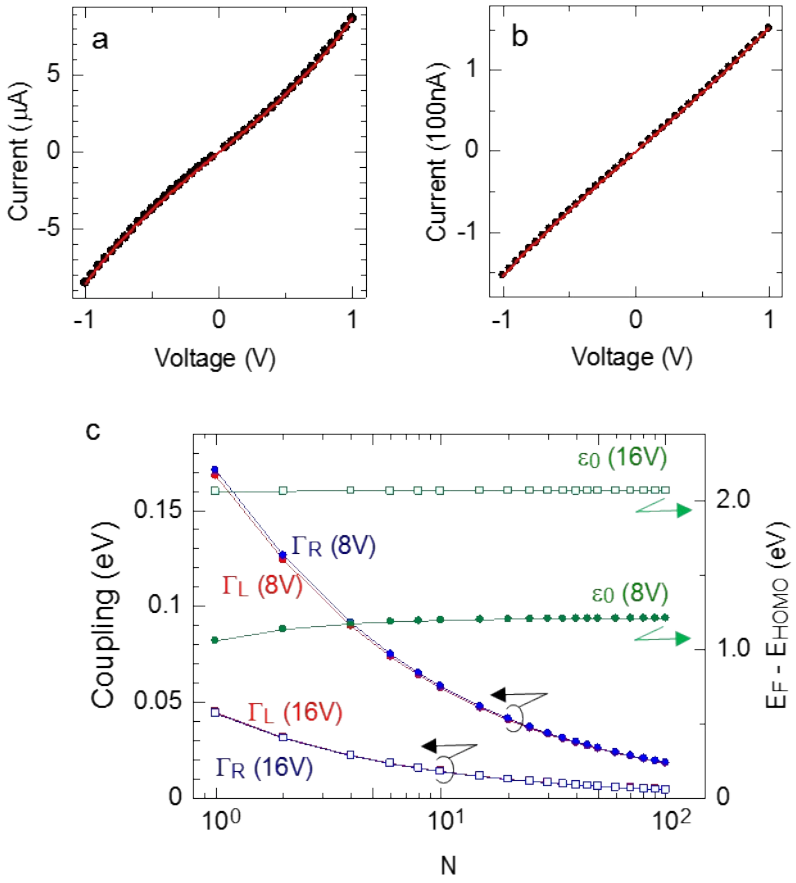


**Fig. S2** Typical *I*–*V* curves obtained using the electrodes formed at process voltages of 8 V (a) and 16 V (b) after immersion in BDT solution. The fits were obtained using Eq. (2). (c) *N* dependences of fitting parameters ($\varepsilon_0$, $\Gamma_L$, and $\Gamma_R$) estimated from the *I*–*V* curves in (a) and (b).

### 3. *I-V* Curve Fitting Using Tunneling Equation

In this study, the *I*–*V* characteristics of nanogap electrodes were investigated using the tunneling equation.[11] In this model, the observed current *I*(*V*) is given by

$$I(V) = \frac{eA}{2\pi hd^2}\left[\left(\phi - \frac{eV}{2}\right)exp\left\{-\frac{4\pi d}{h}\sqrt{2m\left(\phi - \frac{eV}{2}\right)}\right\} - \left(\phi + \frac{eV}{2}\right)exp\left\{-\frac{4\pi d}{h}\sqrt{2m\left(\phi + \frac{eV}{2}\right)}\right\}\right], \quad (1)$$

where *I(V)* is tunnelling current; $e = 1.60 \times 10^{-19}$; $h = 6.62 \times 10^{-34}$; $m = 9.11 \times 10^{-31}$; and *V*, *d*, *A*, and $\phi$ denote the applied voltage, the gap width, the tunnelling emission area, and the barrier height, respectively. Fig. S3a, S3b, and S3c shows the typical experimental and fitted *I*–*V* curves of nanogap electrodes fabricated with process voltages of 8, 10, and 12 V, respectively. These *I-V* curves were selected in Fig. 2a. Table S1 listed the average and standard deviation values of resistance measured at 0.1 V, *d*, *A*, and $\phi$.

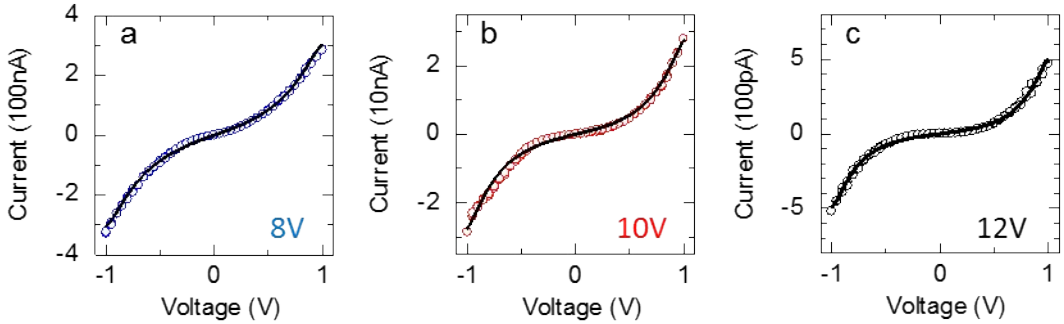


**Fig. S3** Typical *I*–*V* curves obtained using the electrodes formed at process voltages of 8 V (a), 10 V (b), and 12 V (c). The fits were obtained using Eq. (1) using *d* = 0.882 nm, *A* = 5.89 nm², and $\phi$ = 0.556 eV for (a), *d* = 0.994 nm, *A* = 0.864 nm², and $\phi$ = 0.551 eV for (b) , and *d* = 1.10 nm, *A* = 0.0228 nm², and $\phi$ = 0.531 eV for (c).

**Table S1**. Averages and standard deviations of resistance measured at 0.1 V (*R*), gap width (*d*), tunnelling emission area (*A*), and barrier height ($\phi$). *d*, *A*, and $\phi$ were estimated using the tunnelling equation.

| $V_{process}$ | 8 V | 10 V | 12 V |
|---|---|---|---|
| *R* (Ω) | 9.61 ± 10.6 M | 79.6 ± 77.4 M | 17.9 ± 22.2 G |
| *d* (nm) | 0.865 ± 0.0347 | 0.915 ± 0.0416 | 0.988 ± 0.219 |
| *A* (nm²) | 13.5 ± 9.42 | 1.86 ± 1.07 | 0.321 ± 0.394 |
| $\phi$ (eV) | 0.563 ± 0.00709 | 0.566 ± 0.0169 | 0.596 ± 0.0730 |

**References**


1 Y. Komoto, S. Fujii, M. Iwane and M. Kiguchi, *J. Mater. Chem. C*, 2016, **4**, 8842.

2 S. Kaneko, D. Murai, S. Marqués-González, H. Nakamura, Y. Komoto, S. Fujii, T. Nishino, K. Ikeda, K. Tsukagoshi and M. Kiguchi, *J. Am. Chem. Soc.*, 2016, **138**, 1294.

3 X. Y. Xiao, B. Q. Xu and N. J. Tao, *Nano Lett.*, 2004*,* **4**, 267.

4 C. Bruot, J. Hihath and N. J. Tao, *Nat. Nanotechnol*., 2012, ***7,*** 35.

5 R. Matsuhita, M. Horikawa, Y. Naitoh, H. Nakamura and M. Kiguchi, *J. Phys. Chem. C,* 2013, **117,** 1791.

6 M. Tsutsui, Y. Teramae, S. Kurokawa and A. Sakai, *Appl. Phys. Lett.*, 2006, **89**, 163111.

7 S. Ghosh, H. Halimun, A. K. Mahapatro, J. Choi, S. Lodha and D. Janes, *Appl. Phys. Lett.,* 2005, **87**, 233509.

8 Y. Kim, T. Pietsch, A. Erbe, W. Belzig and E. Scheer, *Nano Lett.*, 2011, **11**, 3734.

9 W. Haiss, C. Wang, R. Jitchati, I. Grace, S. Martín, A. S. Batsanov, S. J. Higgins, M. R. Bryce, C. J. Lambert, P. S. Jensen and R. J. Nichols, J*. Phys.: Condens. Matter.*, 2008, **20**, 374119.

10 M. Taniguchi, M. Tsutsui, K. Yokota and T. Kawai, *Nanotechnology*, 2009, **20**, 434008.

11 J. G. Simmons, *J. Appl. Phys.*, 1963, **34**, 2581.